On the Efficiency of the Advanced TWA Approach to the 60-GHz Microstrip Antenna Analysis for 5G Wireless Communication Systems

Mohamed Ayari
Faculty of Computing and Information Technology, Northern Border University, Saudi Arabia | Syscom Laboratory, National Engineering School of Tunis, University of Tunis El-Manar, Tunisia
mohamed.ayari@nbu.edu.sa
(corresponding author)

Received: 21 December 2022 | Revised: 5 January 2023 | Accepted: 7 January 2023

ABSTRACT

The bandwidth demand in mobile wireless applications has grown at an astounding rate due to the fast evolution of technology, spurring the antenna design fields. The approaches associated with realizing antenna structure at mm-Wave frequency bands for future 5G cellular devices present advantages and disadvantages. This paper exhibits a fast and original approach based on the transverse wave formulation called-up Advanced Transverse Wave Approach (ATWA). A compact 5G patch antenna is designed, measured, simulated, and analyzed in the context of unlicensed mm-wave ISM-band applications. Compared to recently published works, the obtained result analysis proves the efficiency of the proposed method in terms of calculation accuracy, computational efficiency, and peak memory usage and the overall good performance of the proposed antenna.

Keywords-5G antennas; advanced transverse wave approach; calculation accuracy, mm-wave analysis

I. INTRODUCTION

Nowadays, much research is directed at the fifth-generation mobile communications system (5G). Soon the traffic volume will be 1000 times over than the last decade with low cost and minimum power consumption, data rate communication will exceed 10Gbps making it 100 times faster than 4G, simultaneous connection of a large number of terminals will be available to support the future spread of M2M communications and internet of things (IoT), all thanks to the 5G technology. Undoubtedly, there are many challenges in this context, among them is to design, treat, and simulate mm-wave antennas used in 5G wireless in an effective way. Numerous recent scientific works have concentrated on the design and mm-wave investigation of 5G antennas with diverse size, from compact to large, either 2D or 3D [1-3]. Besides, 5G antenna shapes (i.e. circular, elliptical, rectangular, hexagonal, cross, etc.) [4-7] are considered as a significant parameter in the analysis process to achieve or not good quality in terms of performance and cost-effectiveness. In wireless communication systems, small patch antennas play an important role in the gain and bandwidth improvements due to features such as multiband properties, low profile topology and cost, good gain, and easy fabrication [8-10].

Several publications have been reported in this context. For instance, a compact size dual band patch antenna functioning at 10.15GHz and 28GHz for 5G mobile communications has been designed and studied in [11]. In [12], the authors presented a new capacitive coupled patch antenna array operating at the frequency band of 24-28GHz providing 360° coverage for 5G based smartphone services. In [13], a patch slotted antenna using FR4 substrate with the size of $18\times18\times1.6\text{mm}^3$ providing at 10.15GHz a gain of 4.46dB and one of 6.6dB at 28GHz was reported in [14] using a small antenna with coplanar feeding for a Rogers RT5880 substrate and $5\times5\times0.254\text{mm}^3$ size. Such antennas present low radiation efficiency, low gain, and some intricacy in the fabrication process. The mm-wave phased array 5G antenna which is running in the frequency range of 25 to 40GHz has been designed and analyzed in the context of Multiple-Input Multiple-Output (MIMO) applications.

The increased demand of frequency allocation coerced the Federal Communication Committee (FCC) to boost more than 18GHz of spectrum surrounding the mm-wave frequencies [15, 43] in order to enhance the development and scientific research in 5G technology. However, the 57-71GHz interval which is the unlicensed frequency band according to FCC covers an important set of applications, such as WiGig [16], a new technology derived from Wi-Fi but supporting faster wireless transfer speed than WiFi. So, many recent publications have been reported in the context of analysis and design of 5G antennas used for WiGig applications. In [17], a stacked circular patch antenna with monopole type pattern was developed for 60GHz WPAN application. A 60GHz microstrip patch antenna was investigated in [18] based on different dielectric materials to prove their impact on antenna operation. In [19], the authors proved the efficiency of a 60GHz virtual loop antenna built on low resistivity silicon substrate. These antennas have been fabricated and designed in different shapes, such as rectangular, circular, helical [20], double F-slot [21], double U-slot [22], T-slot [23], E- and H-slots [24]. Moreover, the feasibility of 5G connectivity beyond 70GHz was demonstrated using an experimental prototype in [25]. The investigation and analysis of mm-wave 5G antenna based on numerical methods is an unprecedented and great challenge in the full-wave electromagnetic (EM) simulation sphere.

Numerical EM methods belong to the core of the mm-wave analysis of 5G planar structures such as the Method Of Moments (MOM) [26], or its alternative Fast Multipole Method (FMM) [27], and the full spectrum method named Partial Element Equivalent Circuit (PEEC)[28] for solving integral equations of EM waves. In the same vein, Finite Element Method (FEM)[29], Finite Difference Time Domain (FDTD) method [30], and Finite Integration Technique (FIT) [31] belong to differential equation solvers. These numerical methods necessitate a significant amount in memory and processor power as well as high accuracy in features and design for full-wave and mm-wave analysis of planar structures employed in wireless systems [32].

In the area of wireless applications, the Advanced Transverse Wave Approach (ATWA) developed by our research team has significant benefits over previous numerical EM approaches in terms of speed, compactness, and memory consumption. To this purpose, we adapt and refine our ATWA approach to work with mm-wave 5G antenna simulations, and we tested its efficiency and stability in this setting. In line with the above mentioned works, an appropriate 5G antenna was considered and designed to validate our approach in the context of mm-wave 5G applications and offer the possibility to investigate smart and powerful antennas for the next generation of innovative wireless technology. In the following, we present and develop our numerical EM method –advanced transverse wave approach– in the context of mm-wave applications.

II. ATWA: THEORETICAL BACKGROUND

For most practical interest problems pertaining to EM radiation and scattering, an analytic solution of integral equations formulating the problem cannot be found. Therefore, researchers tend to utilize computational techniques to obtain a solution. We briefly present in this section the mathematical background and the theoretical foundation of the numerical EM method ATWA as well as its main characteristics and strong points.

The two-dimensional transverse wave approach – a fast numerical method based on an iterative process– has several potentialities that set it apart from other computational EM approaches. There are no matrix inversion calculations in the TWA process, no constraints are required on the component forms, no numerical instabilities frequently arising from large matrices can be found, and the convergence is guaranteed independently of the interfaces of studied planar structures. In the following, we present a small theoretical background of our EM-approach 2D-ATWA for mmWave analysis of planar structures.

The general integral relation linking the electric field to current density and considering the boundary and edge conditions on sub-domains characterizing the air-dielectric interface *Ω* can be written as follows:

$$E(u,v) = \int_S G(u,v,u',v')J(u',v')du'dv' \qquad (1)$$

where $G(u,v,u',v')$ denotes the dyadic Green's function [33].

Referring to the wave concept already investigated and developed in [36], the general equation linking the transverse electric field ET to the transverse magnetic field HT can be expressed as:

$$W_{i,\tau} = (4Z_{0i})^{-\frac{1}{2}}\left(E_{T,i} + (-1)^{\tau} Z_{0i} J_{T,i}\right) \qquad (2)$$

where τ is a Boolean parameter referring to the wave nature (i.e. τ=0 for incident wave (W=A) and τ=1 for reflected wave (W=B)), the superscript T refers to the tangential components, and Z_{0i} stands for the wave impedance of the homogeneous isotropic region $i \in \{1,2\}$ given by:

$$Z_{0i} = \eta_0 \times \left({\mu_{r_i}}/{\varepsilon_{r_i}}\right)^{1/2} \qquad (3)$$

where η_0 is the intrinsic impedance of free space defined as:

$$\eta_0 = 120\pi \text{ or } 377\Omega \qquad (4)$$

where $\varepsilon_{r_i}, \mu_{r_{i,}}$ denote the relative permittivity (capacitivity) and relative permeability (inductivity) of the medium I and the vector J_T is defined from the tangential magnetic field H_T phased by $\pi/2$ from v which denotes the outgoing normal vector oriented towards region i. It can be written as:

$$J_T = H_T \times v \qquad (5)$$

Overall, both incident (A) and reflected (B) waves can be associated through the following relation:

$$\begin{cases} A = \hat{\Gamma} B & \text{In modal domain} \\ B = \hat{S}A + \overset{(0)}{B} & \text{In spatial domain} \end{cases} \qquad (6)$$

where $\overset{(0)}{B}$ represents the general excitation wave on the source.

Moreover, shifting from spatial to modal spaces is guaranteed by the transitional spectral space. In fact, at the discontinuity interface, the two-dimensional Fast Fourier Transform (2D-FFT) or the two-dimensional Non-Uniform Fast Fourier Transform (2D-NUFFT) [37-38] for uniform and non-uniform distribution, respectively, are intercepted in the transition between the spatial and spectral domains in order to accelerate the iterative process. The change from spectral to modal spaces can be ensured by the rotation of angle θ, given by:

$$\theta = arctg(\overset{x}{K}_{mn}/\overset{y}{K}_{mn}) \qquad (7)$$

Undoubtedly, the passing from modal to spatial domains is achieved by the inverse 2D-FFT or 2D-NUFFT as a first step and the rotation of angle$-\theta$ as the next step. The round trip from these spaces is repeated until the system's convergence. The 2D-TWA can be accelerated by applying the anisotropic mesh technique [39] which calls the 2D-NUFFT to manage precisely the non-uniform discretization. Memory and computational complexity for both the Forward and Backward of the ATWA process is guaranteed at $O(N_T logN_T)$ time, where N_T represents the meshing density applied to the structure to be analyzed, whereas the overall computational complexity of iterative solvers is $O(N^2)$, the same with MOM- and FEM-based solvers [40]. Table I recapitulates the iterative process of the ATWA approach, highlighting at each step the computational effort and the total time efficiency.

TABLE I. ITERATIVE PROCESS AND COMPUTATIONAL EFFORT OF ATWA

Step	Description	Complexity
Init	Computation of spectral-modal transition, reflection, and diffraction coefficients. Input complex vectors of bilateral excitation source (incident and reflected waves at *t*=0) $B_0 \neq 0$ and A_0=0.	$\boldsymbol{O(N_T)}$
1	Application of 2D-FFT/2D-NUFFT at iteration *k*.	$\boldsymbol{O(N_T\ logN_T)}$
2	Application of modal transform at iteration *k*.	$\boldsymbol{O(N_T)}$
3	Application of reflection operator at iteration *k*+1.	$\boldsymbol{O(N_T)}$
4	Application of the inverse modal transform at iteration *k*+1.	$\boldsymbol{O(N_T)}$
5	Application of the inverse of 2D-FFT/2D-NUFFT at iteration *k*+1	$\boldsymbol{O(N_T\ logN_T)}$
6	Application of diffraction operator at iteration *k*+1.	$\boldsymbol{O(N_T)}$
7	Compute current density, electric field, and input impedance *Zin* at iteration *k*+1.	$\boldsymbol{O(N_T)}$
8	Test the convergence of *Zin* at iteration *k*+1. If *Zin* converges, then keep all EM quantities Else goto Step 1.	$\boldsymbol{O(N_{Sce})}$ ($N_{Sce} \ll N_T$: total number of pixels on the sub-domain source)

III. ANTENNA DESIGN FOR 5G

The new 5G demand can open prospects for miscellaneous new applications and the design process can be evolved taking into consideration these requirements. Against this background, a 5G small patch antenna fed by a microstrip line has been designed in the context of wireless applications (Figure 1). Such an antenna can enhance the radiation directivity and be used to fix and relay signals around obstacles in the context of ISM-band applications. The proposed planar structure is composed by an $l_p \times w_p$ radiating patch printed upon an $l_s \times p_s \times h_s$ substrate with Rogers 5880. RT/duroid 5880 laminate is considered as a judicious choice and a perfect substrate, since it is isotropic and characterized by the lowest electrical loss for reinforced polytetrafluoroethylene (PTFE) [34], uniform electrical properties over frequency, low moisture absorption, and excellent chemical resistance. This substrate is more convenient to mm-wave applications, military radar systems, commercial airline broadband, and missile guidance systems.

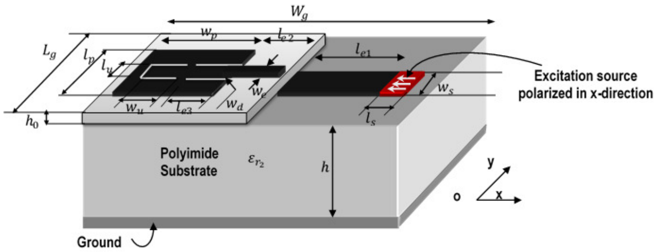

Fig. 1. The proposed 5G small patch antenna fed by microstrip line.

TABLE II. GEOMETRIC SIMULATION PARAMETERS OF THE PROPOSED 5G-ANTENNA

Meshing resolution	512×512
Box dimensions (mm)	$L_g = 8.192$
	$W_g = 8.192$
Patch	Length l_p = 2.912 = 182 pixels
	Width w_p = 3.2 = 200 pixels
Microstrip line (mm)	l_{e1} = 2.56 = 160 pixels
	l_{e2} = 0.96 = 60 pixels
	l_{e3} = 1.12=70 pixels
	w_e = 0.736=46 pixels
U-slot simensions (mm)	l_u = 1.12 = 70 pixels
	w_u = 1.024 = 64 pixels
Width w_d (mm)	w_d = 0.192 = 12 pixels
Source dimensions (mm)	l_s = 0.736 = 46 pixels
	w_s = 1.792 = 112 pixels
Form factor of source	${l_s}/{w_s}$ = 0.41
Substrate	Thickness δ = 130µm
	Type: Rogers RT/duroid
	Height h = 0.5mm

In order to enhance the capacitance inhibiting the probe inductance which causes an expansion of the impedance bandwidth, the U-slot has been loaded on the patch. The U-slot technique has been applied in many recent 5G structures [15, 35] showing adeptness in wideband notion. The design parameters are detailed in Table II.

IV. SIMULATION RESULTS AND DISCUSSION

This section provides a concise and precise description of the experimental results, their interpretation, and the conclusions that can be drawn.

In order to validate our numerical method in the EM simulation space of 5G antennas, we investigate the proposed planar structure shown in Figure 1 by analyzing the S11 parameter and comparing it with the results obtained in the literature. The simulation investigation was carried out by our EM simulator based on the ATWA method and developed in C++ environment. The modeling simulation constraints are given in Table III.

The advanced TWA approach gives certain significant potentialities to the iterative scheme. It detaches the continuities relations defining the boundary conditions from the integral one, taking into consideration the half-spaces describing the different metallic interfaces identifying the proposed structure. One of these potentialities are the above mentioned Heaviside functions associated to the 5G-antenna (i.e. sub-domains: metallic $H_{\Omega_{SUB}} = Me$, dielectric $H_{\Omega_{SUB}} =$

Di, source $H_{\Omega_{SUB}} = Sce$, and surface impedance $H_{\Omega_{SUB}} = I_{surf}$). The reflection coefficient or insertion parameter S11 is considered as the standard parameter for antennas. It quantifies the power reflected from the antenna and identifies the different resonance frequencies. The simulation result as depicted in Figure 2 shows the evolution of the S11 of our proposed antenna.

TABLE III. MODELING SIMULATION PARAMETERS OF THE PROPOSED 5G-ANTENNA

Modeling parameters	Description
Nature of box	Periodic walls
Type of polarization	Bilateral in x-direction
Number of iterations	$N_{iter} = 500$
Value of surface impedance	$Z_S = 0$ (surface impedance sub-domain is equivalent to metallic sub-domain)
Permittivity of regions	$\varepsilon_{r_1} = 1$
	$\varepsilon_{r_2} = 2.2$
Waveband	$F_{min} = 50$GHz
	$F_{max} = 70$GHz
	$Step_F_{rq} = 0.5$Ghz
Height h_0	$h_0 = 0$ (monolayer)

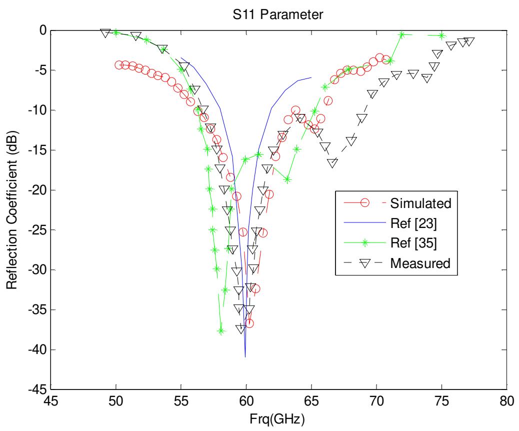

Fig. 2. Evolution of S11 coefficient.

Two bands have been detected at [57.62, 63.32] GHz and [64.29, 66.05] GHz, where the resonance frequencies are respectively depicted at 60.47GHz and 65.17GHz. The return losses are correspondingly -37.83dB and -12.44dB. The Fractional Bandwidths (FBWs) [36] are consequently 9.43% for the first and 2.7% for the second band of the proposed 5G-antenna. The Voltage Standing Wave Ratio (VSWR) is deduced at 1.0260dB for the 60GHz band which is considered as a good impedance for 5G wireless systems. The presence of double resonances is due to the U-slot loaded on the patch antenna that it is warranted by simulation result based on 2D-ATWA. Table III illustrates the comparison between the proposed 5G antenna and other known antennas.

It is noticed that the three selected reference 60GHz antennas are simulated using the Finite-Element Method (FEM)-based Frequency Domain Solver (FDS) of CST Microwave Technology [41] and the FEM based high-frequency structure simulator (HFSS) of ANSYS [24, 42]. Besides, different simulation results of the proposed antenna based on our ATWA method are successfully presented such as the evolution of the impedance as a function of frequency (Figure 3), making evident the stability of the system around the resonance frequency, the 3D-radiation pattern (Figure 4), the azimuth pattern (Figure 5), and the elevation pattern (Figure 6) at 60GHz proving the high and accurate radiation directivity and gain of the proposed 5G antenna.

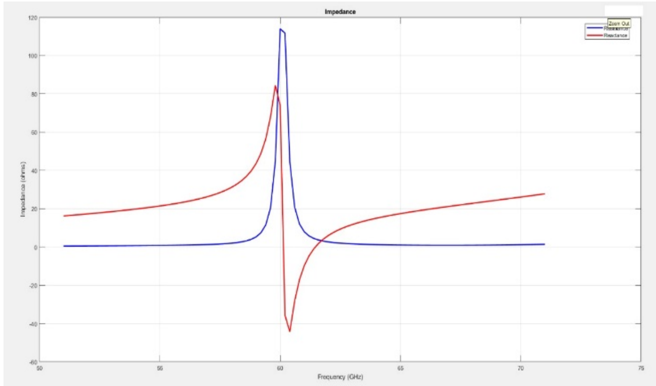

Fig. 3. Evolution of the impedance as a function of frequency.

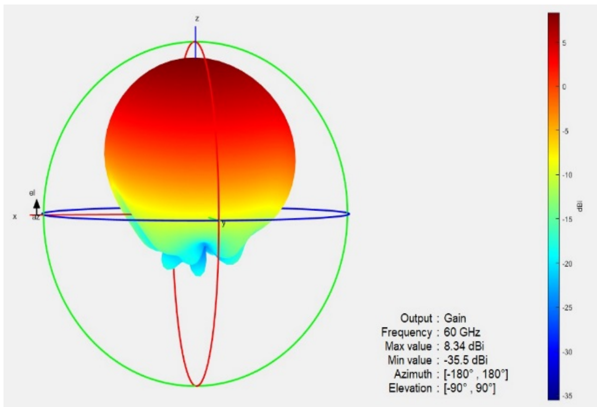

Fig. 4. Radiation pattern at 60GHz.

Overall, the obtained simulation results are in good agreement with the results of [24, 41, 42], with some preferences of our system in terms of size, multi-band notion, and impedance bandwidth. The computational statistics in terms of memory and CPU time for these simulations, using an Intel® Core™ i7-10875H Processor with 8 cores based on the Comet Lake architecture, are given in Table IV. The peak memory usage and total calculation time are significantly reduced in comparison with the other FEM-based solvers with the same computing resources. This proves the feasibility, plausibility, and EM-validity of our approach in 5G antenna simulations along with its accuracy and numerical stability in the compilation process.

In addition, considering the above mentioned features as the efficiency of the AMT technique presented by our approach (ATWA), a good workspace can be opened to investigate miniaturized and sensible structures used for new 5G wireless technologies.

TABLE IV. COMPARISON BETWEEN THE PROPOSED 5G-ANTENNA AND REFERENCE ANTENNAS

	Antenna			
Parameter	**Proposed**	**[24]**	**[41]**	**[42]**
Substrate	RT/duroid 5880	RT/duroid 5880	RT/duroid 5880	RT/duroid 5880
Shape-slot	U-slot	E and H slots	U-slot	U-slot
Size (mm^2)	8.192×8.192	8×8	7.5×9.5	7.5×9.5
Simulator	Own simulator	HFSS	FDS	HFSS
Numerical EM method	ATWA	FEM	FEM	FEM
Return loss (db)	-37.83	-40.99	-37.5	-29.36
Single/multiband	Double band	Single band	Double band	Single band
Impedance bandwidth (dB)	$S_{11} \leq -10$	$S_{11} \leq -10$	$S_{11} \leq -15$	$S_{11} \leq -15$
VSWR at 60GHz band (dB)	1.0260	1.0186	1.0270	1.038
Peak memory usage/GB	6.96	9.53	11.41	10.31

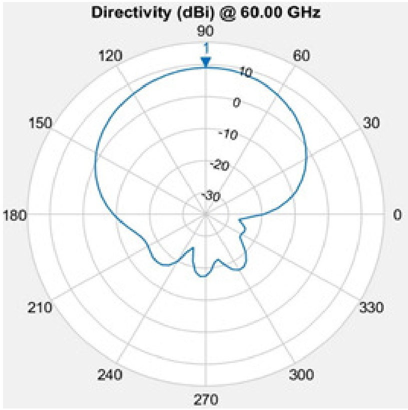

Fig. 5. Azimuth pattern at 60GHz.

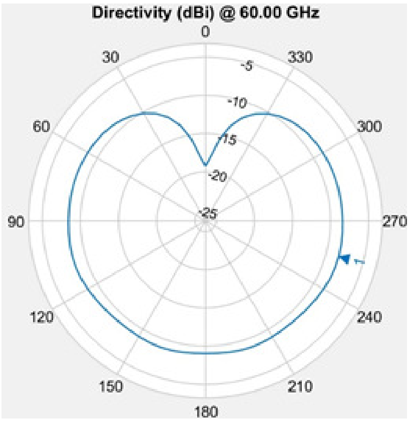

Fig. 6. Elevation pattern at 60GHz.

V. CONCLUSIONS

In this paper, a brief theoretical background and the mathematical foundations of our two-dimensional Advanced Transverse Wave Approach (2D-ATWA) has been presented and developed for mm-wave applications. A 5G small patch antenna with U-slot fed by microstrip line was presented and effectively designed taking into account the presence of the U-shaped slot etched in the radiating patch and the isotropic substrate RT/duroid 5880. The obtained simulations were validated, evaluated, and compared to various 60GHz reference antennas already simulated and investigated using the Finite Element Method-based Frequency Domain Solver and ANSYS HFSS. The results prove the EM-stability and efficiency of our approach in the context of mm-wave applications. Many antenna parameters such as shape, size, embedded shape-slots and slits, substrate material, dimensions, etc. have great impact on the operation of an antenna, such as increasing/decreasing bandwidth and gain or generating single or multiband frequencies. The marriage of numerical EM approaches with the game theory which is considered as a new trend in electromagnetics research can provide efficient solutions to stabilize and select good parameters for rigorous EM-investigation, mainly in the context of mm-wave applications.

REFERENCES

[1] W. A. Awan, S. I. Naqvi, A. H. Naqvi, S. M. Abbas, A. Zaidi, and N. Hussain, "Design and Characterization of Wideband Printed Antenna Based on DGS for 28 GHz 5G Applications," *Journal of Electromagnetic Engineering and Science*, vol. 21, no. 3, pp. 177–183, Jul. 2021, https://doi.org/10.26866/jees.2021.3.r.24.

[2] D. T. T. My, H. N. B. Phuong, T. T. Huong, and B. T. M. Tu, "Design of a Four-Element Array Antenna for 5G Cellular Wireless Networks," *Engineering, Technology & Applied Science Research*, vol. 10, no. 5, pp. 6259–6263, Oct. 2020, https://doi.org/10.48084/etasr.3771.

[3] H. Alsaif, "Compact Hexagonal Monopole Antenna for Lower 5G Bands," *Engineering, Technology & Applied Science Research*, vol. 9, no. 3, pp. 4200–4202, Jun. 2019, https://doi.org/10.48084/etasr.2714.

[4] A. Jamil, K. Rafique, M. D. Idrees, A. S. Rajput, A. Abdullah, and A. S. Saand, "Design and Geometric Transformations of Koch Curve Monopole Antennas," *Engineering, Technology & Applied Science Research*, vol. 12, no. 2, pp. 8452–8457, Apr. 2022, https://doi.org/10.48084/etasr.4767.

[5] G.-H. Jeon, P. A. Dzagbletey, and J.-Y. Chung, "A Cross-Joint Vivaldi Antenna Pair for Dual-Pol and Broadband Testing Capabilities," *Journal of Electromagnetic Engineering and Science*, vol. 21, no. 3, pp. 201–209, Jul. 2021, https://doi.org/10.26866/jees.2021.3.r.27.

[6] D. V. Nandalal, A. Pavithra, S. Pavithra, and M. Kalaiselvi, "Performance Measure of Ultra wide Band Antenna for Hexagonal and Rectangular Shape for Wearable Application," *Asian Journal of Applied Science and Technology*, vol. 1, no. 3, pp. 80–84, 2017.

[7] M. J. Hakeem and M. M. Nahas, "Improving the Performance of a Microstrip Antenna by Adding a Slot into Different Patch Designs," *Engineering, Technology & Applied Science Research*, vol. 11, no. 4, pp. 7469–7476, Aug. 2021, https://doi.org/10.48084/etasr.4280.

[8] M. Nahas, "A Super High Gain L-Slotted Microstrip Patch Antenna For 5G Mobile Systems Operating at 26 and 28 GHz," *Engineering, Technology & Applied Science Research*, vol. 12, no. 1, pp. 8053–8057, Feb. 2022, https://doi.org/10.48084/etasr.4657.

[9] S. Nelaturi and N. V. S. N. Sarma, "Compact Wideband Microstrip Patch Antenna based on High Impedance Surface," *Engineering, Technology & Applied Science Research*, vol. 8, no. 4, pp. 3149–3152, Aug. 2018, https://doi.org/10.48084/etasr.1971.

[10] D. Imran *et al.*, "Millimeter wave microstrip patch antenna for 5G mobile communication," in *International Conference on Engineering*

and Emerging Technologies, Lahore, Pakistan, Feb. 2018, pp. 1–6, https://doi.org/10.1109/ICEET1.2018.8338623.

[11] Y. Jandi, F. Gharnati, and A. Oulad Said, "Design of a compact dual bands patch antenna for 5G applications," in *International Conference on Wireless Technologies, Embedded and Intelligent Systems*, Fez, Morocco, Apr. 2017, pp. 1–4, https://doi.org/10.1109/WITS.2017.7934628.

[12] M. Stanley, Y. Huang, H. Wang, H. Zhou, A. Alieldin, and S. Joseph, "A Capacitive Coupled Patch Antenna Array With High Gain and Wide Coverage for 5G Smartphone Applications," *IEEE Access*, vol. 6, pp. 41942–41954, 2018, https://doi.org/10.1109/ACCESS.2018.2860795.

[13] N. Kalwit, P. Pawar, and P. Moghe, "Microstrip Patch Antenna for Future 5G Applications," in *Mobile Radio Communications and 5G Networks*, N. Marriwala, C. C. Tripathi, D. Kumar, and S. Jain, Eds. Singapore, Asia: Springer, 2021, pp. 469–474.

[14] O. M. Haraz, M. M. M. Ali, S. Alshebeili, and A.-R. Sebak, "Design of a 28/38 GHz dual-band printed slot antenna for the future 5G mobile communication Networks," in *International Symposium on Antennas and Propagation & USNC/URSI National Radio Science Meeting*, Vancouver, BC, Canada, Jul. 2015, pp. 1532–1533, https://doi.org/10.1109/APS.2015.7305155.

[15] A. Morgado, K. M. S. Huq, S. Mumtaz, and J. Rodriguez, "A survey of 5G technologies: regulatory, standardization and industrial perspectives," *Digital Communications and Networks*, vol. 4, no. 2, pp. 87–97, Apr. 2018, https://doi.org/10.1016/j.dcan.2017.09.010.

[16] M. S. Ibrahim, "Low-Cost, Circularly Polarized, and Wideband U-Slot Microstrip Patch Antenna with Parasitic Elements for WiGig and WPAN Applications," in *13th European Conference on Antennas and Propagation*, Krakow, Poland, Mar. 2019, pp. 1–4.

[17] W. Byun, B.-S. Kim, K.-S. Kim, M.-S. Kang, and M.-S. Song, "Stacked circular patch antenna with monopole type pattern for 60GHz WPAN application," in *IEEE Antennas and Propagation Society International Symposium*, San Diego, CA, USA, Jul. 2008, pp. 1–4, https://doi.org/10.1109/APS.2008.4620014.

[18] M. Kamran Saleem, M. Xie, M. A. S. Alkanhal, and M. Saadi, "Effect of dielectric materials on integrated lens antenna for millimeter wave applications," *Microwave and Optical Technology Letters*, vol. 61, no. 4, pp. 1079–1083, 2019, https://doi.org/10.1002/mop.31676.

[19] D. Bereka, A. Gopinath, and B. Sainati, "Design of a 60GHz high efficiency virtual loop antenna on low resistivity silicon substrate," in *IEEE International Symposium on Antennas and Propagation*, Spokane, WA, USA, Jul. 2011, pp. 891–894, https://doi.org/10.1109/APS.2011.5996419.

[20] C. Liu, Y.-X. Guo, X. Bao, and S.-Q. Xiao, "60-GHz LTCC Integrated Circularly Polarized Helical Antenna Array," *IEEE Transactions on Antennas and Propagation*, vol. 60, no. 3, pp. 1329–1335, Mar. 2012, https://doi.org/10.1109/TAP.2011.2180351.

[21] F. Ahmad and B. Tlili, "Design and analysis of millimeter wave double F slot patch antenna for future 5G wireless communication," in *International Conference on Electrical and Computing Technologies and Applications*, Ras Al Khaimah, United Arab Emirates, Nov. 2017, pp. 1–4, https://doi.org/10.1109/ICECTA.2017.8252049.

[22] T. H. Jang, H. Y. Kim, D. M. Kang, S. H. Kim, and C. S. Park, "60 GHz Low-Profile, Wideband Dual-Polarized U-Slot Coupled Patch Antenna With High Isolation," *IEEE Transactions on Antennas and Propagation*, vol. 67, no. 7, pp. 4453–4462, Jul. 2019, https://doi.org/10.1109/TAP.2019.2911623.

[23] R. K. Goyal and K. K. Sharma, "T-slotted microstrip patch antenna for 5G Wi-Fi network," in *International Conference on Advances in Computing, Communications and Informatics*, Jaipur, India, Sep. 2016, pp. 2684–2687, https://doi.org/10.1109/ICACCI.2016.7732465.

[24] J. Saini and S. K. Agarwal, "Design a single band microstrip patch antenna at 60 GHz millimeter wave for 5G application," in *International Conference on Computer, Communications and Electronics (Comptelix)*, Jaipur, India, Jul. 2017, pp. 227–230, https://doi.org/10.1109/COMPTELIX.2017.8003969.

[25] G. Hattab, E. Visotsky, M. Cudak, and A. Ghosh, "Toward the Coexistence of 5G MmWave Networks with Incumbent Systems beyond 70 GHz," *IEEE Wireless Communications*, vol. 25, no. 4, pp. 18–24, Aug. 2018, https://doi.org/10.1109/MWC.2018.1700436.

[26] M. Ayari, Y. E. Touati, and S. Altowaijri, "Method of Moments versus Advanced Transverse Wave Approach for EM Validation of Complex Microwave and RF Applications," *Journal of Electromagnetic Engineering and Science*, vol. 20, no. 1, pp. 31–38, Jan. 2020, https://doi.org/10.26866/jees.2020.20.1.31.

[27] B. Wu and X.-Q. Sheng, "Fast Characteristic Mode Analysis for Half-space Platform Antennas with Multilevel Fast Multipole Algorithm," in *International Applied Computational Electromagnetics Society Symposium - China*, Beijing, China, Jul. 2018, pp. 1–2, https://doi.org/10.23919/ACESS.2018.8669181.

[28] C.-C. Chou and T.-L. Wu, "Direct Simulation of the Full-Wave Partial Element Equivalent Circuit Using Standard SPICE [Application Notes]," *IEEE Microwave Magazine*, vol. 20, no. 6, pp. 22–34, Jun. 2019, https://doi.org/10.1109/MMM.2019.2904376.

[29] H. Santos, P. Pinho, and H. Salgado, "Patch Antenna-in-Package for 5G Communications with Dual Polarization and High Isolation," *Electronics*, vol. 9, no. 8, Aug. 2020, Art. no. 1223, https://doi.org/10.3390/electronics9081223.

[30] K. R. Mahmoud and A. M. Montaser, "Design of Compact mm-wave Tunable Filtenna Using Capacitor Loaded Trapezoid Slots in Ground Plane for 5G Router Applications," *IEEE Access*, vol. 8, pp. 27715–27723, 2020, https://doi.org/10.1109/ACCESS.2020.291606.

[31] A. Rahimian, S. F. Jilani, Q. H. Abbasi, A. Alomainy, and Y. Alfadhl, "A Millimetre-Wave Two-Dimensional 64-Element Array for Large-Scale 5G Antenna Subsystems," in *13th European Conference on Antennas and Propagation*, Krakow, Poland, Mar. 2019, pp. 1–2.

[32] D. He, B. Ai, K. Guan, L. Wang, Z. Zhong, and T. Kürner, "The Design and Applications of High-Performance Ray-Tracing Simulation Platform for 5G and Beyond Wireless Communications: A Tutorial," *IEEE Communications Surveys & Tutorials*, vol. 21, no. 1, pp. 10–27, 2019, https://doi.org/10.1109/COMST.2018.2865724.

[33] A. Eroglu and J. K. Lee, "Dyadic Green's functions for an electrically gyrotropic medium," *Progress in Electromagnetics Research*, vol. 58, pp. 223–241, 2006, https://doi.org/10.2528/PIER05070203.

[34] T. Itoh, "Spectral Domain Immitance Approach for Dispersion Characteristics of Generalized Printed Transmission Lines," *IEEE Transactions on Microwave Theory and Techniques*, vol. 28, no. 7, pp. 733–736, Apr. 1980, https://doi.org/10.1109/TMTT.1980.1130158.

[35] M. Titaouine, A. G. Neto, H. Baudrand, and F. Djahli, "WCIP method applied to active frequency selective surfaces," *Journal of Microwaves, Optoelectronics and Electromagnetic Applications*, vol. 6, no. 1, pp. 1–16, Aug. 2007.

[36] H. Baudrand, M. K. Azizi, and M. Titaouine, "General Principles of the Wave Concept Iterative Process," in *The Wave Concept in Electromagnetism and Circuits: Theory and Applications*, New York, NY, USA: Wiley, 2016, pp. 1–42.

[37] M. Ayari, T. Aguili, H. Temimi, and H. Baudrand, "More efficiency of Transverse Wave Approach (TWA) by applying Anisotropic Mesh Technique (AMT) for full-wave analysis of microwave planar structures," *Progress In Electromagnetics Research B*, vol. 14, pp. 383–405, Jan. 2009.

[38] M. Ayari, T. Aguili, and H. Baudrand, "New Version of Twa Using Two-Dimensional Non-Uniform Fast Fourier Mode Transform (2D-Nuffmt) for Full-Wave Investigation of Microwave Integrated Circuits," *Progress In Electromagnetics Research B*, vol. 15, pp. 375–400, 2009, https://doi.org/10.2528/PIERB09052301.

[39] M. Ayari, T. Aguili, H. Temimi, and H. Baudrand, "On the Use of Anisotropic Mesh Technique (AMT) in Transverse Wave Approach (TWA) for the EM Analysis of Microwave Circuits in Wireless Applications," in *Symposia and Workshops on Ubiquitous, Autonomic and Trusted Computing*, Brisbane, QLD, Australia, Jul. 2009, pp. 246–251, https://doi.org/10.1109/UIC-ATC.2009.8.

[40] S. Zuo, D. Garcia Donoro, Y. Zhang, Y. Bai, and X. Zhao, "Simulation of Challenging Electromagnetic Problems Using a Massively Parallel Finite Element Method Solver," *IEEE Access*, vol. 7, pp. 20346–20362, 2019, https://doi.org/10.1109/ACCESS.2019.2896615.

[41] H. Liu, Y. He, and H. Wong, "Printed U-slot patch antenna for 60GHz applications," in *International Workshop on Electromagnetics, Applications and Student Innovation Competition*, Kowloon, Hong Kong, Aug. 2013, pp. 153–155, https://doi.org/10.1109/iWEM.2013.6888796.

[42] G. Kumar and C. Kumar, "Design and analysis of u-slot mircostrip patch antenna for mobile communication at 60 ghz," *Acta Technica Corviniensis - Bulletin of Engineering*, vol. 13, no. 1, pp. 35–38, 2020.

[43] S. Ahmad *et al.*, "Design of a Tri-Band Wearable Antenna for Millimeter-Wave 5G Applications," *Sensors*, vol. 22, no. 20, Jan. 2022, Art. no. 8012, https://doi.org/10.3390/s22208012.

AUTHOR PROFILE

Mohamed Ayari –received the Dipl.-Ing., M.S., and Ph.D. degrees in Telecommunications in 2003, 2004, and 2009, respectively, from the National Engineering School of Tunis (ENIT), Tunisia, in collaboration with the National Polytechnic Institute of Toulouse, France, and Virginia Tech, USA. He has been teaching at several universities since 2003. He has been a permanent research member at the 6'COM laboratory at ENIT from 2003. In 2005, he joined RCEM-Inc. in Toulouse, France. Since 2010, he has been a tenure-track Associate Professor at the National Engineering School of Carthage (ENICAR), Carthage University, Tunisia. In 2015, he joined the IT Department of the Faculty of Computing and Information Technology, Northern Border University (NBU), Kingdom of Saudi Arabia, as an Assistant Professor. His current research interests are electromagnetic (EM) fields, numerical EM methods, and computer-aided design of microwave circuits and antennas. His research interests also include information security, image processing and wireless applications.